Aerosol and Air Quality Research
January 2016, Volume 16, Issue 1, Pages 46-60
http://dx.doi.org/10.4209/aaqr.2015.04.0219
http://archimer.ifremer.fr/doc/00276/38769/

Seasonal Variations of Total Gaseous Mercury at a French Coastal Mediterranean Site

Marusczak Nicolas [1, *], Castelle Sabine [1], De Vogue Benoist [1], Knoery Joel [2], Cossa Daniel [1]

[1] IFREMER, Centre de Méditerranée, CS 20330, F-83507, La Seyne-sur-Mer, France
[2] IFREMER, Centre Nantes, BP 21109, F-44311, Nantes, France

* Corresponding author : Nicolas Marusczak, Tel: +33 (0)5 61 33 26 07 ; Fax: +33 (0)5 61 33 28 88 ; email address : nicolas.marusczak@get.obs-mip.fr

Abstract :

The seasonal variation and spatial distribution of atmospheric particles at three islands in the Taiwan Strait were investigated. Atmospheric particles (PM10) were collected at three offshore islands (i.e., Kinmen islands, Matsu islands, and Penghu Islands) and two coastal regions (i.e., Xiamen and Fuzhou) in the years of 2008–2012. Field sampling results indicated that the average PM10 concentrations at the Kinmen islands were generally higher than other sampling sites, suggesting that a superimposition phenomenon was regularly observed during the air pollution episodes at Kinmen Islands and Xiamen region. PM10 samples were analyzed for their chemical composition, including water-soluble ions, metallic elements, and carbonaceous content. The most abundant water-soluble ionic species of PM10 were recognized as SO42–, NO3–, and NH4+, indicating that PM10 was mainly composed of secondary inorganic aerosols. Although natural crustal elements dominated the metallic content of PM10, the most abundant anthropogenic metals of PM10 were Zn and Pb. Enrichment factor calculations showed that Ni, Cr, and Zn were the enriched elements emitted mainly from anthropogenic sources. Moreover, the OC concentration of PM10 was always higher than that of EC at all sampling sites. High OC/EC ratios of PM10 were commonly observed at the sampling sites on the Matsu Islands, the Fuzhou region, and the Penghu Islands. Source apportionment results indicated that vehicular exhausts were the main source of PM10, and followed by industrial boilers, secondary aerosols, soil dusts, biomass burning, petrochemical plants, steel plants, oceanic spray, and cement plants at the island and coastal sampling sites in the Taiwan Strait.

Highlights

► Investigation of 2 years of TGM at a French coastal Mediterranean site. ► Daily variations of TGM are observed, due to local industrial or urban activities. ► Seasonal variations are due to the dispersion of pollutants in the troposphere. ► High TGM concentrations are due to air masses coming from local or regional sources.

Keywords : Total gaseous mercury, Coastal Mediterranean site, Anthropogenic and local sources, Seasonal and daily variations

1. INTRODUCTION

The atmosphere is an environmental compartment where volatile chemical contaminants reside before being deposited on soil and water surfaces. Therefore, it plays an important role in the dispersion of volatile pollutants over the Earth's surface. This is particularly the case for mercury (Hg), a toxic heavy metal widely distributed in the atmosphere in elemental and divalent volatile forms (Selin *et al.*, 2007). Hg is emitted to the atmosphere from both natural (Ferrara *et al.*, 2000b) and anthropogenic (Pirrone *et al.*, 2001) sources. Gaseous Elemental Mercury (GEM) is the predominant form of Hg (95 %) in the boundary layer with a residence time of about 6-24 months (Lamborg *et al.*, 2002; Slemr *et al.*, 2003), permitting its long range transport. GEM is subsequently oxidized to divalent mercury species (Hg(II)), including reactive gaseous oxidized mercury (GOM : $HgCl_2$, $HgBr_2$, $Hg(OH)_2$, etc.) and particulate bound Hg (PBM). GOM and PBM deposit rapidly (days-weeks) to continental surfaces and contaminate a variety of environments including soil, snow and water (Hammerschmidt *et al.*, 2006; Poissant *et al.*, 2008; Amos *et al.*, 2012).

The Hg cycle has been widely perturbed by human activities (Fitzgerald *et al.*, 2007; Lamborg *et al.*, 2014), and the anthropogenic component of Hg in the atmosphere is currently around 30% (Pirrone *et al.*, 2010). However, Hg evasion from the sea surface will still remain an important source of Hg in the atmosphere for a long period of time, because of the quantity of the Hg legacy and the size of the reservoir (Ferrara *et al.*, 2000a). In particular, the Atlantic Ocean and European seas have an influence on atmospheric Hg concentrations in the European troposphere, especially at coastal sites. For example, Kock *et al.,* (2005) have compared long-term trends of atmospheric Hg concentrations at two coastal monitoring stations (Mace Head, Ireland and Zingst, Germany) and observed that, in addition to a seasonal signal, their measurements revealed northern hemispheric background values. The authors also showed that GEM concentration in

Mace Head (1.72 ng.m^{-3}) is 0.06 ng.m^{-3} higher than those of Zingst (1.66 ng.m^{-3}). This difference would probably be due to differences in local emissions from the sea surface, because no anthropogenic mercury source exists near Mace Head station. Photoreduction of dissolved Hg(II), which is the main pathway for GEM production in natural surface waters (Amyot *et al.*,, 1997), is clearly at the origin of this process. Thus, coastal and oceanic sites are of great interest in observing both marine and continental atmospheric Hg dynamics. These observations are essential in calibrating regional and global Hg cycling models that can subsequently be used to simulate the impact of environmental policy scenarios on global Hg deposition. Several international programs for monitoring atmospheric Hg exist, *e.g.* Atmospheric Mercury network: AMNet, European Monitoring and Evaluation Program: EMEP, Global mercury Observation system: GMOS, Canadian Atmospheric Mercury Measurement Network: CAMNET). In this context, several projects have been devoted to the Mediterranean Sea over the last twenty years: (MAMCS: Mediterranean Atmospheric Mercury Cycle System, MOE: Mercury Species over Europe and MERCYMS: An Integrated Approach to Assess the Mercury Cycle in the Mediterranean Basin). The Mediterranean Sea elicits a particular interest for studying the Hg cycle, since it is a semi-enclosed basin, under the influence of European and African continental inputs. The basin is sensitive and reactive to climatic and environmental changes (Bethoux *et al.*,, 1999), which may affect Hg deposition and evasion (Durrieu de Madron *et al.*,, 2011). Apart from the work by Wangberg *et al.,* (2008), performed within the framework of the MERCYMS project, continuous monitoring of atmospheric Hg in the Mediterranean troposphere is lacking. The present study provides two-years of continuous measurements of total gaseous mercury (TGM) at a Northwestern Mediterranean coastal site (La Seyne-sur-Mer, France). The objective was to identify marine and continental Hg sources with the aid of several atmospheric environmental tracers (NO_X, CO, O_3, PM10, and meteorological parameters).

METHODS

Site description

All measurements were performed at La Seyne-sur-Mer, on the southeastern coast of France (43° 6'21.06"N, 5°53'7.78"E) (Fig 1.) and situated within 5 kilometers of Toulon city center. Toulon is a large urban area with approximately half a million inhabitants. Toulon hosts a commercial harbor and naval base with few industries, and one municipal waste incinerator situated in the urban area. All measuring instruments are 15 meters above sea level, 500 meters away from the closest secondary road and about 2 km from a large highway. La Seyne-sur-Mer is characterized by a Mediterranean climate: hot dry summers and mild and relatively wet winters. Winds come principally from the North-North-West or South-South-West, whereas La Seyne-sur-Mer is sheltered and protected from the North by the mountainous “massif des Maures” (780m asl). Sometimes, there is a wind of East-South-East, often bringing rainfall. In summer, most of winds are from south (marine origin), while in winter winds come from North-North-West (continental area).

TGM measurements

Two different analyzers have been used to measure TGM. From January 2009 to December 2009, TGM was measured directly and continuously, using a portable automated Mercury analyzer Gardis-5 (UAB Tikslioji technika, Lituania), which provides a measurement every 10 minutes. The analyzer is described in detail elsewhere (Urba *et al.*,, 1995). Briefly, air is pumped through a single gold trap where atmospheric mercury is amalgamated and retained. Every 10 minutes, amalgamated mercury is desorbed and detected by cold vapor atomic absorption spectrometry (CVAAS). Ambient air (pumped at a 200 mL/min flow rate) was pre-filtered (0.45 µm pore size,

LCR Millipore) to prevent the entry of particulate matter into the measurement system. The filter was changed every two weeks and instrumental sensitivity controlled daily and automatically with several injections from an external calibration unit (Model GA-730 Mercury Vapor Dosing Unit).

The second instrument was used from January to December, 2012. Measurements of TGM were carried out using a Tekran Model 2537A (Tekran Inc., Canada). The analytical technique (CVAFS) is based on the collection of ambient mercury onto two gold traps, followed by thermal desorption and final detection by cold vapor atomic fluorescence spectrometry (CVAFS). The time resolution was 5 min, the sampling flow rate was 1.5 $L.min^{-1}$ and the analyzer was self-calibrated every 47 hours by an internal Hg permeation source. A 47 mm diameter Teflon filter (pore size 0.45 µm) is placed in front of the sample line to prevent the entry of particles into the system. This filter was changed every 2 weeks. An intercomparison of these two instruments was made by Munthe *et al.* (2001) and has shown that the results are comparable (Munthe *et al.*,, 2001).

Meteorological, chemical parameters and statistics

Meteorological data were collected with a weather station located at La Seyne-sur-Mer, close to the sampling site. The station measured atmospheric temperature (T), air pressure (AP), and humidity (RH). Regarding wind speed (WS) and wind direction (WD) we have use the regional mesoscale model MM5 (Grell *et al.*,, 1994) of the Pennsylvania State University. Different chemical parameters were also measured at La Seyne-sur-Mer (Air-PACA) including nitrogen oxides (NOx), ozone (O_3) and particulate matter inferior at 10µm (PM10). NOx was measured by chemiluminescence (Model 200E, Teledyne instrument), O_3 by UV absorption (Model O341M, Environnement S.A.) and PM10 by quartz microbalance (Model BAM-1020, Met One

Instruments). Carbon monoxide (CO) has been measured by IR absorption (Model T300U, Teledyne instrument). In order to assess the impact of meteorological parameters, three-day back-trajectories were used to identify air mass origins during the sampling period in this study. The three days backward trajectories were calculated using the NOAA HYSPLIT 4 with the EDAS (Eta Data Assimilation System) meteorological data and vertical mixing model. Arrival heights of 500 meters (m), 150 m and 15 m were used to describe the regional meteorological patterns.

All statistical analyses were carried out using JMP 10 software (SAS Institute). Correlation analysis was carried out using a correlation matrix. Statistical significance was determined for a probability of $\alpha<0.05$. A statistical summary of all chemical and meteorological parameters is presented in Table 1.

Quality assurances and quality control procedure

Both instrument have an automatic calibration step with an internal mercury permeation source for Tekran instrument and an external calibration unit (Model GA-730 Mercury Vapor Dosing Unit) for Gardis instrument. All data and all maintenance were treated by a QA/QC procedure with a software program developed by the LGGE (Laboratoire de Glaciologie et Géophysique de l'Environnement). QA/AC procedure is describe by Angot *et al.*, (2014).

RESULTS AND DISCUSSION

Average concentration and seasonal variations of TGM

Ambient TGM concentrations ranged from 1.15 to 5.73 $ng.m^{-3}$ (average 2.20 ± 0.54 $ng.m^{-3}$) in 2009 and from 1.19 to 6.15 $ng.m^{-3}$ (average 2.16 ± 0.60 $ng.m^{-3}$) in 2012. The ambient concentrations of TGM from 16th January 2009 to 31st December 2009 and from 16th January 2012 to 31st December 2012 at La Seyne-sur-Mer are shown in Fig.2. These values are roughly

30 % more elevated than the global background concentration in the Northern Hemisphere (1.75 ng m^{-3} in 1996–1999 to about 1.4 ng m^{-3} in 2009) (Lindberg *et al.*,, 2007; Slemr *et al.*,, 2011). High annual averages and frequent occurrence of pollution events (Fig.2) suggest that a large proportion of the measurements are not background concentrations. These results are somewhat higher than those observed at another Mediterranean coastal site (EMEP station Cabo de Creus in Spain, Thau Lagoon in France, Piran in Slovenia, Lucido in Italia and Neve Yam in Israel) by Wängberg *et al.* (2008), with TGM observed concentrations of 1.75-1.8 ng.m^{-3}, but similar to other studies at coastal sites in the world with a TGM concentration from 1.6 ng.m^{-3} to 2.4 ng.m^{-3} (Wangberg *et al.*,, 2001) or with TGM concentration of 2.55 ng.m^{-3} (Zhijia Ci *et al.*,, 2011) . These average concentrations of TGM are higher that other TGM measurements in northern Europe (Munthe *et al.*,, 2001) confirming that TGM concentrations are higher in the Mediterranean region than in the Northern Europe, where industrials and urban areas are more numerous (Pirrone *et al.*,, 2001; Kotnik, 2013).

We observed a seasonal variation in TGM concentration, with a maximum of 2.51 ± 0.44 ng.m^{-3} in winter (Dec-Feb) and minimum of 1.95 ± 0.53 ng.m^{-3} in summer (Jun-Aug) for 2009 and a maximum of 2.43 ± 0.72 ng.m^{-3} in winter and a minimum of 1.97 ± 0.57 ng.m^{-3} in autumn (Sept-Nov) for 2012 (Fig.3). The influence of different meteorological and atmospheric chemical parameters on TGM concentrations for each season and each year were investigated. A multivariate analysis (Table 2) shows that TGM concentrations were negatively correlated with wind speed factor for each season of each year (2009 : winter r = -0.39; spring, r = -0.04; summer, r = -0.25; fall, r = -0.17. 2012 : winter r = -0.41; spring, r = -0.19; summer, r = -0.29; fall, r = -0.43.). This suggests that the seasonal TGM concentration observed at La Seyne-sur-Mer are not due to TGM inputs from wind transport of terrestrial or marine origin but a local production of TGM. This statement was verified by analyzing the influence of atmospheric chemical

parameters (CO, O_3, NOx and PM10) for each season. However, it is possible that with a high wind speed, mixing of air masses is greater, and thus a dilution of TGM and other pollutant within the boundary layer. Furthermore, the multivariate analysis (Table 2) shows that for each season of both years, TGM concentrations were significantly correlated with other chemical parameters. This seasonal phenomenon is common to several air pollutants and explained as the result of the dispersion of pollutants in the boundary layer, due to changes in air mass stratification with temperature. The atmospheric boundary layer is thicker in summer due to greater solar radiation, which promotes convection, and, thus, a better dispersion of Hg in thicker atmospheric layers. In addition, we observe a significant positive correlation between TGM and CO in winter for both year ($r=0.16$; $p<0.0001$ for 2009 and $r=0.46$; $p<0.0001$ for 2012), and it is known that domestic heating using the combustion of fossil fuels, can intensify atmospheric emissions during winter (CO and TGM), when the atmospheric mixing layer is thinner (Kock *et al.*,, 2005). If we compare seasonal TGM and O_3 variations, we observe a significant negative correlation for each season of each year (2009: winter r = -0.54; spring, r = -0.32; summer, r = -0.34; fall, r = -0.44. 2012: winter r = -0.42; spring, r = -0.44; summer, r = -0.53; fall, r = -0.58.). Indeed, O_3 is maximal in summer and minimal in winter, while TGM is minimal in summer and maximal in winter. It is known that the tropospheric ozone concentrations are higher in summer than in winter, due to a stronger solar radiation and thus a higher O_3 production in the summer. Indeed, tropospheric ozone is formed primarily by photochemical reactions involving pollutants emitted by human activities, including nitrogen oxides (NOx) and volatile organic compounds (VOCs). A high O_3 concentration reflects a strong atmospheric oxidant potential. A strong atmospheric oxidant potential can cause a possible higher GEM oxidation to GOM by radical •OH or halogens compounds (Br, BrO), which is rapidly deposited and seen in the

217 decrease in TGM. Thereby TGM concentration may decrease in summer due to a strong potential
218 atmospheric oxidation between GEM and GOM.
219 An another explanation to confirm this TGM seasonality, is the fact that is exist a seasonal
220 variation of the origin of air masses which arrive at La Seyne-sur-Mer, and generally in this part
221 of coastal Mediterranean. Indeed, in summer the majority of air masses have a marine origin
222 (South South-Est), while in winter the air masses come essentially from north north-west, with a
223 continental origin. As well, a marine air mass is less contaminated in mercury than a continental
224 air mass. Indeed, Kotnik *et al*. (2013) show that the TGM concentration over the Mediterranean
225 Sea is lower (1.6 – 1.9 $ng.m^{-3}$) than TGM measurements at La Seyne-sur-Mer. This observation
226 and this correlation could explain also this seasonal variation. This situation is opposite from that
227 described in Wängberg et al. (2008). They compared atmospheric Hg concentrations at five other
228 coastal Mediterranean sites, and observed an opposite seasonal cycle with maxima in summer and
229 minima in winter. They attributed these variations to TGM evasion from the sea surface. Their
230 measurements were conducted during 4 field campaigns of 15 days each season. We can infer
231 from these diverging observations that local and regional atmospheric conditions are able to
232 generate various types of seasonality in the TGM atmospheric signal. La Seyne-sur-Mer and
233 more generally the urban area of Toulon, with numerous activities (naval and tourist port,
234 militaries activity) play a strong role in the TGM concentration with a seasonal patterns primarily
235 due to the anthropogenic activities of the urban area.
236
237 ***Daily variations of TGM.***
238
239 Fig. 4 illustrates the daily variation in TGM at La Seyne-sur-Mer for 2012, averaged over both
240 monitoring years. TGM maxima occur in the early morning and minima in the middle of the
241 afternoon during all seasons. Two hypotheses can be put forward to explain these daily TGM
242 variations: (i) daily solar radiation variation, inducing a daily cycle in the amplitude of the

243 photoreduction of Hg(II) from surface waters and soils; and/or (ii) the daily cycle of the urban or
244 industrial activities around the observation site. At La Seyne-sur-Mer for daily-averaged
245 observations, covariations of TGM and other monitored atmospheric pollutants are observed. For
246 example, Fig. 5 shows the variation of TGM, O_3, NO_X, CO and PM 10 in December 2012. We
247 observed that TGM, NO_X, CO and PM10, exhibit the same pattern during December 2012. Most
248 of observed increases of CO, NOX, PM10 and TGM occur together, from the middle of afternoon
249 to noon the next day (4:00 pm to 12:00 pm). This observation reflected that TGM is directly in
250 relationship with these anthropogenic pollutants. These pollutants are essentially produced by
251 motor traffic (NOx) and fossil fuel combustion (CO, and PM 10) and are considered as tracers of
252 local pollution. O_3 also is affected by the high concentration of NOx as NO oxidation consumes,
253 and thereby lowers, O_3 to produce NO_2. The diurnal variation of TGM can thus be affected by the
254 combination of local chemical reaction, natural/anthropogenic sources, mixing height variation,
255 and transport. Also, the combustion of fossil fuel (for domestic heating) could increase the
256 concentration of TGM, NOx and other compounds in the atmosphere. For example, from 11th
257 December 2012 at 4:00 p.m. to 12th December at 3:00 p.m., mercury concentrations increased
258 progressively and strongly to a maximum of 2.22 $ng.m^{-3}$ at 9:00 a.m. Conversely, the atmospheric
259 temperature has experienced a sharp decline to reach 1.3°C on 12th December at 4:00 a.m.
260 However, it is highly likely that with these temperatures, the consumption of fossil fuels for
261 domestic heating has increased. This results in a net increase in the concentrations of CO and
262 PM10 that are two tracers of anthropogenic and local emissions. Thus, it appears that the daily
263 variations of TGM during this period are principally due to the cyclic activity of urban and
264 industrial activities near the sampling site. The hypothesis of a natural origin for the daily
265 variations is not supported by our results. While a marine origin of TGM cannot be ruled out, we

suggest that in coastal regions impacted by industrial and urban areas, anthropogenic Hg emissions may be the main factor controlling the daily variations in TGM concentrations.

Air masses affecting TGM concentrations

To improve the insights and understanding of TGM concentrations measured at La Seyne-sur-Mer, we analyzed correlations between meteorological parameters (wind direction, wind speed, humidity, dew point and temperature) and TGM concentrations. The wind directions presented in Fig.6a and Fig.6b show that at La Seyne-sur-Mer most winds came from North-North-West and South-South-West for both years. These wind directions show that the majority of the air masses passing over the sampling site in 2009 and 2012 have a continental imprint. In particular the air masses passing over the Marseille-Aix-en-Provence urban area, with its 1.7 million inhabitants, and those from the Rhone valley. Winds from the East were also observed for both years, and are often linked to rain events in the area.

Multivariate correlation analysis (Table 2) shows that TGM is not significantly correlated with wind direction ($r=-0.02$; $p=0.4603$ for 2009 and $r=0.15$; $p<0.0209$ for 2012) but a significant negative correlation between wind speed and TGM exists ($r=-0.08$; $p=0.0005$ for 2009 and $r=-0.37$; $p<0.0001$ for 2012). These observations confirm that a local production of TGM is predominant, compared to a long range transport of TGM. However, if we consider high concentrations of TGM (> 3 ng.m^{-3}), Fig. 7 shows that they were predominantly observed with a light breeze from West-South-West sector for both years and with an average of wind speed of 3.5 m.s^{-1} for 2009 and 3.2 m.s^{-1} for 2012. These averages of wind speed correspond to a Beaufort class of 2, so a light breeze. This confirms that all TGM concentration superior at 3 ng.m^{-3} come from probably of a local production by industries or urban area. However, we observe that concentrations of TGM superior at 3 ng.m^{-3} coming from West (North-West and South-West)

represent 69% for 2009 and 86% for 2012 for all measurements like show by the TGM rose (Fig.7). These sectors correspond to the “Mistral” wind. “Mistral” is a cold and strong wind coming from the Rhône Valley (North of La Seyne-sur-Mer) and then, which spreads to eastern in direction to Toulon. These air masses are very much imprinted either by the Rhône-Valley or the Marseille-Aix urban and industrial area. Both can have a strong influence on TGM concentration, and especially because of the many anthropogenic and human activities. To verify this, we have simulated three days back trajectories (Fig.8) with a new trajectory every 3 hours when an episode of high significant concentration of TGM (> 3 $ng.m^{-3}$) was observed for either year (18th June 2009, 06:00 am; 05th July 2009, 06:00 am; 14th February 2012, 06:00 pm; 07th September 2012). We show that all simulated back trajectory have air masses with a continental origin and particularly imprinted by the Rhone Valley or the Marseille-Aix urban and industrial area. This observation confirms the fact that the high concentrations of TGM (> 3 $ng.m^{-3}$) have also a continental and anthropogenic origin and are transported by these air masses. In short, we show that the highest TGM concentrations occur during (i) ”Mistral” wind periods, draining the influence of anthropogenic Hg inputs from the Rhone Valley and the Marseille-Aix area and/or (ii) during the wind is very low (Beaufort Classes 2) confirming a local production of TGM. Consequently, the highest concentrations of TGM (> 3 $ng.m^{-3}$) measured at La Seyne-sur-Mer are mainly due to industrial or urban activities and thus to regional activities.

CONCLUSIONS

This study investigated TGM concentrations at a coastal Mediterranean site (La Seyne-sur-Mer) in relation to other atmospheric pollutants (CO, O_3, NO_X and PM10) and meteorological parameters. We show that seasonal and daily cycles are superimposed on the regional TGM background. The seasonal variations of TGM show maximum levels in winter and minimum

316 levels in summer, associated with the variation of other atmospheric contaminants (CO, NO_X and
317 PM10). Daily TGM variation correlates with cyclic urban and industrial activities in the area,
318 suggesting the influence of anthropogenic emissions even in coastal regions. This anthropogenic
319 influence is both local (when winds are weak) and regional under the northerly wind ("Mistral")
320 regime, which saw the highest TGM concentrations (> 3ng.m^{-3}) observed at the study site. Above
321 a background concentration level at this coastal site, observed variations of TGM are mainly due
322 to local and regional anthropogenic sources.

323

324 **ACKNOWLEDGMENTS**
325
326 This work is part of the Global Mercury Observation System (GMOS) project financed by the
327 European Union in the 7th Framework Programme under contract N°265113. Monitoring in 2009
328 was supported by the Agence National de la Recherche (ANR EXTREMA, ANR-06-VULN-005)
329 and by the Agence de l'Eau Rhône Méditerranée Corse (project ARC-MED). We would like to
330 thank AirPACA for atmospheric chemical pollutant data, S. Coudray and C. Tomasino (Ifremer
331 LER/PAC, La Seyne-sur-Mer) for meteorological data and drafting Fig. 1, respectively. Special
332 thanks to A. Dommergue and M. Barret for their help regarding TGM data QA/AC.

333

334 **REFERENCES**
335
336
337 Amos, H.M., Jacob, D.J., Holmes, C.D., Fisher, J.A., Wang, Q., Yantosca, R.M., Corbitt, E.S., Galarneau, E., Rutter,
338 A.P., Gustin, M.S., Steffen, A., Schauer, J.J., Graydon, J.A., St Louis, V.L., Talbot, R.W., Edgerton, E.S.,
339 Zhang, Y. and Sunderland, E.M. (2012). Gas-Particle Partitioning of Atmospheric Hg(Ii) and Its Effect on
340 Global Mercury Deposition. *Atmos Chem Phys* 12: 591-603.
341 Amyot, M., Gill, G.A. and Morel, F.M.M. (1997). Production and Loss of Dissolved Gaseous Mercury in Coastal
342 Seawater. *Environmental Science & Technology* 31: 3606-3611.
343 Angot, H., Barret, M., Magand, O., Ramonet, M. and Dommergue, A. (2014). A 2-Year Record of Atmospheric
344 Mercury Species at a Background Southern Hemisphere Station on Amsterdam Island. *Atmos Chem Phys*
345 14: 11461-11473.
346 Bethoux, J.P., Gentili, B., Morin, P., Nicolas, E., Pierre, C. and Ruiz-Pino, D. (1999). The Mediterranean Sea: A
347 Miniature Ocean for Climatic and Environmental Studies and a Key for the Climatic Functioning of the
348 North Atlantic. *Prog Oceanogr* 44: 131-146.
349 Durrieu de Madron, X., Guieu, C., Sempéré, R., Conan, P., Cossa, D., D'Ortenzio, F., Estournel, C., Gazeau, F.,
350 Rabouille, C., Stemmann, L., Bonnet, S., Diaz, F., Koubbi, P., Radakovitch, O., Babin, M., Baklouti, M.,
351 Bancon-Montigny, C., Belviso, S., Bensoussan, N., Bonsang, B., Bouloubassi, I., Brunet, C., Cadiou, J.F.,

352 Carlotti, F., Chami, M., Charmasson, S., Charrière, B., Dachs, J., Doxaran, D., Dutay, J.C., Elbaz-Poulichet,
353 F., Eléaume, M., Eyrolles, F., Fernandez, C., Fowler, S., Francour, P., Gaertner, J.C., Galzin, R., Gasparini,
354 S., Ghiglione, J.F., Gonzalez, J.L., Goyet, C., Guidi, L., Guizien, K., Heimbürger, L.E., Jacquet, S.H.M.,
355 Jeffrey, W.H., Joux, F., Le Hir, P., Leblanc, K., Lefèvre, D., Lejeusne, C., Lemé, R., Loÿe-Pilot, M.D.,
356 Mallet, M., Méjanelle, L., Mélin, F., Mellon, C., Mérigot, B., Merle, P.L., Migon, C., Miller, W.L., Mortier,
357 L., Mostajir, B., Mousseau, L., Moutin, T., Para, J., Pérez, T., Petrenko, A., Poggiale, J.C., Prieur, L., Pujo-
358 Pay, M., Pulido, V., Raimbault, P., Rees, A.P., Ridame, C., Rontani, J.F., Ruiz Pino, D., Sicre, M.A.,
359 Taillandier, V., Tamburini, C., Tanaka, T., Taupier-Letage, I., Tedetti, M., Testor, P., Thébault, H.,
360 Thouvenin, B., Touratier, F., Tronczynski, J., Ulses, C., Van Wambeke, F., Vantrepotte, V., Vaz, S. and
361 Verney, R. (2011). Marine Ecosystems' Responses to Climatic and Anthropogenic Forcings in the
362 Mediterranean. *Prog Oceanogr* 91: 97-166.
363 Ferrara, R., Mazzolai, B., Lanzillotta, E., Nucaro, E. and Pirrone, N. (2000a). Temporal Trends in Gaseous Mercury
364 Evasion from the Mediterranean Seawaters. *Science of The Total Environment* 259: 183-190.
365 Ferrara, R., Mazzolai, B., Lanzillotta, E., Nucaro, E. and Pirrone, N. (2000b). Volcanoes as Emission Sources of
366 Atmospheric Mercury in the Mediterranean Basin. *Science of The Total Environment* 259: 115-121.
367 Fitzgerald, W.F., Lamborg, C.H. and Hammerschmidt, C.R. (2007). Marine Biogeochemical Cycling of Mercury.
368 *Chemical Reviews* 107: 641-662.
369 Grell, G., J. Dudhia and Stauffe, a.D. (1994). A Description of the Fifth Generation Penn State/Ncar Mesoscale
370 Model (Mm5). *NCAR Tech. Note NCAR/TN-398 1 STR*: 177 pp.
371 Hammerschmidt, C.R., Fitzgerald, W.F., Lamborg, C.H., Balcom, P.H. and Tseng, C.M. (2006). Biogeochemical
372 Cycling of Methylmercury in Lakes and Tundra Watersheds of Arctic Alaska. *Environ Sci Technol* 40:
373 1204-1211.
374 Kock, H.H., Bieber, E., Ebinghaus, R., Spain, T.G. and Thees, B. (2005). Comparison of Long-Term Trends and
375 Seasonal Variations of Atmospheric Mercury Concentrations at the Two European Coastal Monitoring
376 Stations Mace Head, Ireland, and Zingst, Germany. *Atmospheric Environment* 39: 7549-7556.
377 Kotnik, J., Sprovieri, F., Ogrinc, O., Horvat, M., Pirrone, N., (2013). Mercury in the Mediterranean, Part I : Spatial
378 and Temporal Trends. *Environ Sci Pollut Res*.
379 Lamborg, C.H., Fitzgerald, W.F., O'Donnell, J. and Torgersen, T. (2002). A Non-Steady State Box Model of Global-
380 Scale Mercury Biogeochemistry with Interhemispheric Atmospheric Gradients. *Abstr Pap Am Chem S* 223:
381 U520-U520.
382 Lamborg, C.H., Hammerschmidt, C.R., Bowman, K.L., Swarr, G.J., Munson, K.M., Ohnemus, D.C., Lam, P.J.,
383 Heimburger, L.E., Rijkenberg, M.J.A. and Saito, M.A. (2014). A Global Ocean Inventory of Anthropogenic
384 Mercury Based on Water Column Measurements. *Nature* 512: 65-+.
385 Lindberg, S., Bullock, R., Ebinghaus, R., Engstrom, D., Feng, X.B., Fitzgerald, W., Pirrone, N., Prestbo, E. and
386 Seigneur, C. (2007). A Synthesis of Progress and Uncertainties in Attributing the Sources of Mercury in
387 Deposition. *Ambio* 36: 19-32.
388 Munthe, J., Wangberg, I., Pirrone, N., Iverfeldt, A., Ferrara, R., Ebinghaus, R., Feng, X., Gardfeldt, K., Keeler, G.,
389 Lanzillotta, E., Lindberg, S.E., Lu, J., Mamane, Y., Prestbo, E., Schmolke, S., Schroeder, W.H., Sommar, J.,
390 Sprovieri, F., Stevens, R.K., Stratton, W., Tuncel, G. and Urba, A. (2001). Intercomparison of Methods for
391 Sampling and Analysis of Atmospheric Mercury Species. *Atmospheric Environment* 35: 3007-3017.
392 Pirrone, N., Cinnirella, S., Feng, X., Finkelman, R.B., Friedli, H.R., Leaner, J., Mason, R., Mukherjee, A.B., Stracher,
393 G.B., Streets, D.G. and Telmer, K. (2010). Global Mercury Emissions to the Atmosphere from
394 Anthropogenic and Natural Sources. *Atmos Chem Phys* 10: 5951-5964.
395 Pirrone, N., Costa, P., Pacyna, J.M. and Ferrara, R. (2001). Mercury Emissions to the Atmosphere from Natural and
396 Anthropogenic Sources in the Mediterranean Region. *Atmospheric Environment* 35: 2997-3006.
397 Poissant, L., Zhang, H.H., Canario, J. and Constant, P. (2008). Critical Review of Mercury Fates and Contamination
398 in the Arctic Tundra Ecosystem. *The Science of the total environment* 400: 173-211.
399 Selin, N.E., Jacob, D.J., Park, R.J., Yantosca, R.M., Strode, S., Jaegle, L. and Jaffe, D. (2007). Chemical Cycling and
400 Deposition of Atmospheric Mercury: Global Constraints from Observations. *J Geophys Res-Atmos* 112.
401 Slemr, F., Brunke, E.-G., Ebinghaus, R., Temme, C., Munthe, J., Wängberg, I., Schroeder, W., Steffen, A. and Berg,
402 T. (2003). Worldwide Trend of Atmospheric Mercury since 1977. *Geophys. Res. Lett.* 30: 1516.
403 Slemr, F., Brunke, E.G., Ebinghaus, R. and Kuss, J. (2011). Worldwide Trend of Atmospheric Mercury since 1995.
404 *Atmos Chem Phys* 11: 4779-4787.
405 Urba, A., Kvietkus, K., Sakalys, J., Xiao, Z. and Lindqvist, O. (1995). A New Sensitive and Portable Mercury-Vapor
406 Analyzer Gardis-1a. *Water Air Soil Poll* 80: 1305-1309.
407 Wangberg, I., Munthe, J., Amouroux, D., Andersson, M.E., Fajon, V., Ferrara, R., Gardfeldt, K., Horvat, M.,
408 Mamane, Y., Melamed, E., Monperrus, M., Ogrinc, N., Yossef, O., Pirrone, N., Sommar, J. and Sprovieri, F.
409 (2008). Atmospheric Mercury at Mediterranean Coastal Stations. *Environ Fluid Mech* 8: 101-116.

410 Wangberg, I., Munthe, J., Pirrone, N., Iverfeldt, A., Bahlman, E., Costa, P., Ebinghaus, R., Feng, X., Ferrara, R.,
411 Gardfeldt, K., Kock, H., Lanzillotta, E., Mamane, Y., Mas, F., Melamed, E., Osnat, Y., Prestbo, E., Sommar,
412 J., Schmolke, S., Spain, G., Sprovieri, F. and Tuncel, G. (2001). Atmospheric Mercury Distribution in
413 Northern Europe and in the Mediterranean Region. *Atmospheric Environment* 35: 3019-3025.
414 Zhijia Ci, Xiaoshan Zhang and Wang, Z. (2011). Elemental Mercury in Coastal Seawater of Yellow Sea, China:
415 Temporal Variation and Airesea Exchange. *Atmospheric Environment* 45: 183-190.

416

Tables

Seasonal variations of total gaseous mercury at a French coastal Mediterranean site

Nicolas Marusczak[1,a*], Sabine Castelle[1], Benoist de Vogüé[1], Joël Knoery[2] and Daniel Cossa[1,b]

[1] IFREMER, Centre de Méditerranée, CS 20330, F-83507, La Seyne-sur-Mer, France
[2] IFREMER, Centre Nantes, BP 21109, F-44311, Nantes, France
[a] Present address, Observatoire Midi-Pyrénées, Laboratoire Géosciences Environnement Toulouse, CNRS/IRD/Université Paul Sabatier Toulouse III, 14 avenue Edouard Belin, 31400 Toulouse, France
[b] Present address, ISTerre, Université J. Fourier, BP 53, F-38041, Grenoble, France

Table 1 : Statistical summary of all parameters (T: Temperature; WS : wind speed, WD: Wind direction; AP: Air pressure; RH: Relative humidity; O_3: Ozone; CO: Carbon monoxide; NOx: Nitrogrn oxyde; PM10: particulate matter inferior at 10µm) for both years, 2009 and 2012.

Table 2a: Multivariate analysis of all parameters (T: Temperature; WS : wind speed, WD: Wind direction; AP: Air pressure; RH: Relative humidity) for each season of 2009. Values statistically significant ($\alpha<0.05$) are shown with an asterisks.

Table 2b: Multivariate analysis of all parameters (T: Temperature; WS : wind speed, WD: Wind direction; AP: Air pressure; RH: Relative humidity) for each season of 2012. Values statistically significant ($\alpha<0.05$) are shown with an asterisks. (N.D. signify No Data).

* Corresponding author. Tel: +33 (0)5 61 33 26 07 ; Fax: +33 (0)5 61 33 28 88

E-*mail address*: nicolas.marusczak@get.obs-mip.fr

2009

	TGM ($ng.m^{-3}$)	**T** (°C)	**WS** ($m.s^{-1}$)	**WD** (°N)	**AP** (hPa)	**RH** (%)	**O_3** ($\mu g.m^{-3}$)	**CO** ($\mu g.m^{-3}$)	**NOx** ($\mu g.m^{-3}$)	**PM10** ($\mu g.m^{-3}$)
n	5602	8399	2799	2799	8399	8399	8255	8255	8255	8389
Aveage	2.2	16.89	4.93	218.14	1013.35	69.32	28.05	386.28	28.59	28.74
Std. Dev	0.54	6.53	3.11	92.26	7.2	16.22	18.51	417.81	40.61	16.6
Min.	1.15	-1.3	0.11	0	980	15	0	0	0	0
Max.	5.73	34.5	16.36	360	1031	97	98.5	2707.42	460.53	124
Median	2.13	16.8	4.46	211	1015	72	28.5	174.67	15.43	26

2012

	TGM ($ng.m^{-3}$)	**T** (°C)	**WS** ($m.s^{-1}$)	**WD** (°N)	**AP** (hPa)	**RH** (%)	**O_3** ($\mu g.m^{-3}$)	**CO** ($\mu g.m^{-3}$)	**NOx** ($\mu g.m^{-3}$)	**PM10** ($\mu g.m^{-3}$)
n	7933	8037	2791	2791	8037	8165	8376	750	8374	7725
Aveage	2.16	17.38	4.82	221.14	1013.5	66.48	28.7	607.21	29.08	30.2
Std. Dev	0.6	7.06	3.2	92.02	18.22	15.07	16.36	160.13	44.04	17.79
Min.	1.19	-2.2	0.1	0	916	23	0	478.8	0	0
Max.	6.16	36.3	21.1	360	1033	94	91.5	1847.8	463.76	139
Median	2.02	17.4	4.2	216	1018	67	29.5	546.62	14.63	29

Table 1 : Statistical summary of all parameters (T: Temperature; WS : wind speed, WD: Wind direction; AP: Air pressure; RH: Relative humidity; O_3: Ozone; CO: Carbon monoxide; NOx: Nitrogrn oxyde; PM10: particulate matter inferior at 10µm) for both years, 2009 and 2012.

Fall

	TGM	T	WS	WD	AP	RH	O_3	CO	NOx	PM10
TGM	1.00*									
T	-0.34*	1.00*								
WS	-0.17*	-0.33*	1.00*							
WD	0.06	-0.41*	0.33*	1.00*						
AP	-0.07	0.48*	-0.42*	-0.33*	1.00*					
RH	0.07*	0.10*	-0.23*	-0.15*	0.23*	1.00*				
O_3	-0.44*	0.44*	0.12*	-0.21*	0.00	-0.19*	1.00*			
CO	0.24*	0.12*	-0.34*	-0.14*	0.15*	0.01	-0.19*	1.00*		
NOx	0.40*	-0.12*	-0.29*	-0.04	0.14*	0.08*	-0.56*	0.53*	1.00*	
PM10	0.37*	0.26*	-0.49*	-0.23*	0.49*	0.27*	-0.29*	0.41*	0.51*	1.00*

Spring

	TGM	T	WS	WD	AP	RH	O_3	CO	NOx	PM10
TGM	1.00*									
T	-0.16*	1.00*								
WS	-0.04	-0.15*	1.00*							
WD	0.04	-0.28*	0.29*	1.00*						
AP	-0.11*	0.20*	-0.27*	-0.20*	1.00*					
RH	0.00	-0.48*	-0.21*	0.04	-0.06*	1.00*				
O_3	-0.32*	0.46*	0.19*	-0.27*	-0.05*	-0.36*	1.00*			
CO	0.06*	0.42*	-0.19*	-0.11*	0.07*	-0.09*	-0.07*	1.00*		
NOx	0.29*	-0.16*	-0.16*	0.05*	0.09*	0.08*	-0.63*	0.33*	1.00*	
PM10	0.09*	0.22*	-0.14*	-0.14*	0.19*	0.04*	-0.08*	0.24*	0.38*	1.00*

Winter

	TGM	T	WS	WD	AP	RH	O_3	CO	NOx	PM10
TGM	1.00*									
T	0.00*	1.00*								
WS	-0.39*	-0.14*	1.00*							
WD	-0.32*	-0.23*	0.36*	1.00*						
AP	0.00*	0.00	-0.39*	0.00	1.00*					
RH	0.31*	-0.02	-0.27*	-0.34*	-0.23*	1.00*				
O_3	-0.54*	0.41*	0.29*	0.09	0.00	-0.35*	1.00*			
CO	0.41*	-0.21*	-0.31*	-0.11*	0.13*	0.25*	-0.62*	1.00*		
NOx	0.46*	-0.23*	-0.31*	-0.09	0.17*	0.15*	-0.60*	0.86*	1.00*	
PM10	0.44*	-0.04	-0.51*	-0.17*	0.40*	0.20*	-0.41*	0.58*	0.57*	1.00*

Summer

	TGM	T	WS	WD	AP	RH	O_3	CO	NOx	PM10
TGM	1.00*									
T	0.03*	1.00*								
WS	-0.25*	-0.02	1.00*							
WD	-0.13*	-0.29*	0.41*	1.00*						
AP	0.03	0.01	-0.27*	-0.20*	1.00*					
RH	0.19*	-0.41*	-0.48*	-0.15*	0.10*	1.00*				
O_3	-0.34*	0.57*	0.06	-0.27*	-0.16*	-0.16*	1.00*			
CO	0.15*	0.14*	-0.27*	-0.17*	0.05*	-0.04	-0.11*	1.00*		
NOx	0.41*	-0.14*	-0.16*	-0.03	0.18*	0.04	-0.55*	0.35*	1.00*	
PM10	0.21*	0.38*	-0.20*	-0.21*	0.07*	0.11	0.16*	0.21*	0.20*	1.00*

Table 2a: Multivariate analysis of all parameters (T: Temperature; WS : wind speed, WD: Wind direction; AP: Air pressure; RH: Relative humidity; O_3: Ozone; CO: Carbon monoxide; NOx: Nitrogrn oxyde; PM10: particulate matter inferior at 10µm) for each season of 2009. Values statistically significant ($\alpha<0.05$) are shown with an asterisks.

Fall

	TGM	T	WS	WD	AP	RH	O_3	CO	NOx	PM10
TGM	1.00*									
T	-0.10*	1.00*								
WS	-0.43*	-0.17*	1.00*							
WD	-0.07	-0.31*	0.25*	1.00*						
AP	0.02	0.11*	-0.13*	0.02	1.00*					
RH	0.37*	0.08*	-0.41*	-0.34*	-0.06*	1.00*				
O3	-0.58*	0.51*	0.33*	-0.10*	0.07*	-0.36*	1.00*			
CO	0.43*	-0.17*	-0.30*	0.03*	0.74*	0.12*	-0.44*	1.00*		
NOx	0.47*	-0.25*	-0.31*	-0.03	0.06*	0.17*	-0.58*	0.55*	1.00*	
PM10	0.48*	0.19*	-0.43*	-0.20*	0.23*	0.26*	-0.26*	0.53*	0.48*	1.00*

Spring

	TGM	T	WS	WD	AP	RH	O_3	CO	NOx	PM10
GEM	1.00*									
T	-0.25*	1.00*								
WS	-0.19*	-0.26*	1.00*							
WD	0.09*	-0.30*	0.36*	1.00*						
AP	-0.27*	0.45*	-0.28*	-0.11*	1.00*					
RH	0.12*	-0.49*	-0.21*	-0.02	-0.14*	1.00*				
O_3	-0.44*	0.57*	0.15*	-0.22*	0.11*	-0.49*	1.00*			
CO	N.D.	N.D.	N.D.	N.D.	N.D.	N.D.	N.D.	N.D.		
NOx	0.34*	-0.02	-0.21*	-0.01	0.02	0.08*	-0.43*	0.00*	1.00*	
PM10	0.15*	0.36*	-0.22*	-0.19*	-0.09*	-0.01	0.09*	0.00*	0.38*	1.00*

Winter

	TGM	T	WS	WD	AP	RH	O_3	CO	NOx	PM10
TGM	1.00*									
T	-0.30*	1.00*								
WS	-0.41*	0.13*	1.00*							
WD	-0.16*	-0.11*	0.29*	1.00*						
AP	0.00	0.30*	-0.22*	-0.13*	1.00*					
RH	0.05*	-0.14*	-0.31*	-0.07	0.32*	1.00*				
O_3	-0.42*	0.48*	0.21*	-0.13*	0.00	-0.15*	1.00*			
CO	0.97*	-0.35*	-0.45*	-0.16	0.05*	0.05*	-0.49*	1.00*		
NOx	0.39*	-0.15*	-0.24*	-0.06	0.04*	-0.15*	-0.50*	0.52*	1.00*	
PM10	0.69*	-0.16	-0.43*	-0.20*	0.17*	0.10	-0.28*	0.73*	0.44*	1.00*

Summer

	TGM	T	WS	WD	AP	RH	O_3	CO	NOx	PM10
TGM	1.00*									
T	-0.36*	1.00*								
WS	-0.29*	-0.11*	1.00*							
WD	0.08*	-0.42*	0.40*	1.00*						
AP	0.14*	0.06*	-0.20*	-0.01	1.00*					
RH	0.41*	-0.47*	-0.31*	0.08	-0.01*	1.00*				
O_3	-0.53*	0.64*	0.08*	-0.24*	0.00	-0.50*	1.00*			
CO	N.D.	N.D.	N.D.	N.D.	N.D.	N.D.	N.D.	N.D.		
NOx	0.34*	-0.06*	-0.31*	-0.11*	0.15*	0.06*	-0.32*	0.00*	1.00*	
PM10	0.23*	0.33*	-0.29*	-0.19*	0.06*	0.12*	0.16*	0.00*	0.39*	1.00*

Table 2b: Multivariate analysis of all parameters (T: Temperature; WS : wind speed, WD: Wind direction; AP: Air pressure; RH: Relative humidity; O_3: Ozone; CO: Carbon monoxide; NOx: Nitrogrn oxyde; PM10: particulate matter inferior at 10µm) for each season of 2012. Statistically significant ($\alpha<0.05$) are shown with an asterisks. (N.D. signify No Data).

Figures

Seasonal variations of total gaseous mercury at a French coastal Mediterranean site

Nicolas Marusczak[1,a*], Sabine Castelle[1], Benoist de Vogüé[1], Joël Knoery[2] and Daniel Cossa[1,b]

[1] IFREMER, Centre de Méditerranée, CS 20330, F-83507, La Seyne-sur-Mer, France
[2] IFREMER, Centre Nantes, BP 21109, F-44311, Nantes, France
[a] Present address, Observatoire Midi-Pyrénées, Laboratoire Géosciences Environnement Toulouse, CNRS/IRD/Université Paul Sabatier Toulouse III, 14 avenue Edouard Belin, 31400 Toulouse, France
[b] Present address, ISTerre, Université J. Fourier, BP 53, F-38041, Grenoble, France

* Corresponding author. Tel: +33 (0)5 61 33 26 07 ; Fax: +33 (0)5 61 33 28 88

E-*mail address*: nicolas.marusczak@get.obs-mip.fr

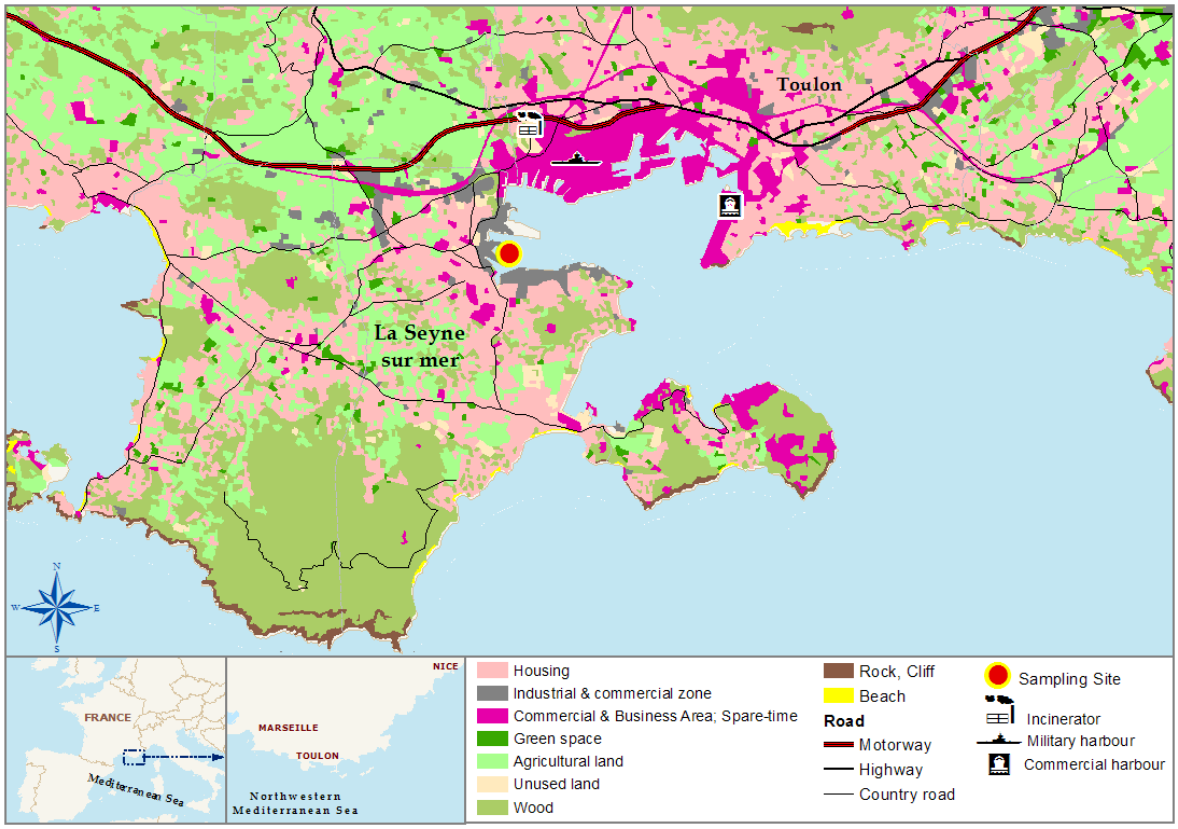

Fig.1: Total gaseous mercury (TGM) sampling site (●) at La Seyne-sur-Mer and its local environment.

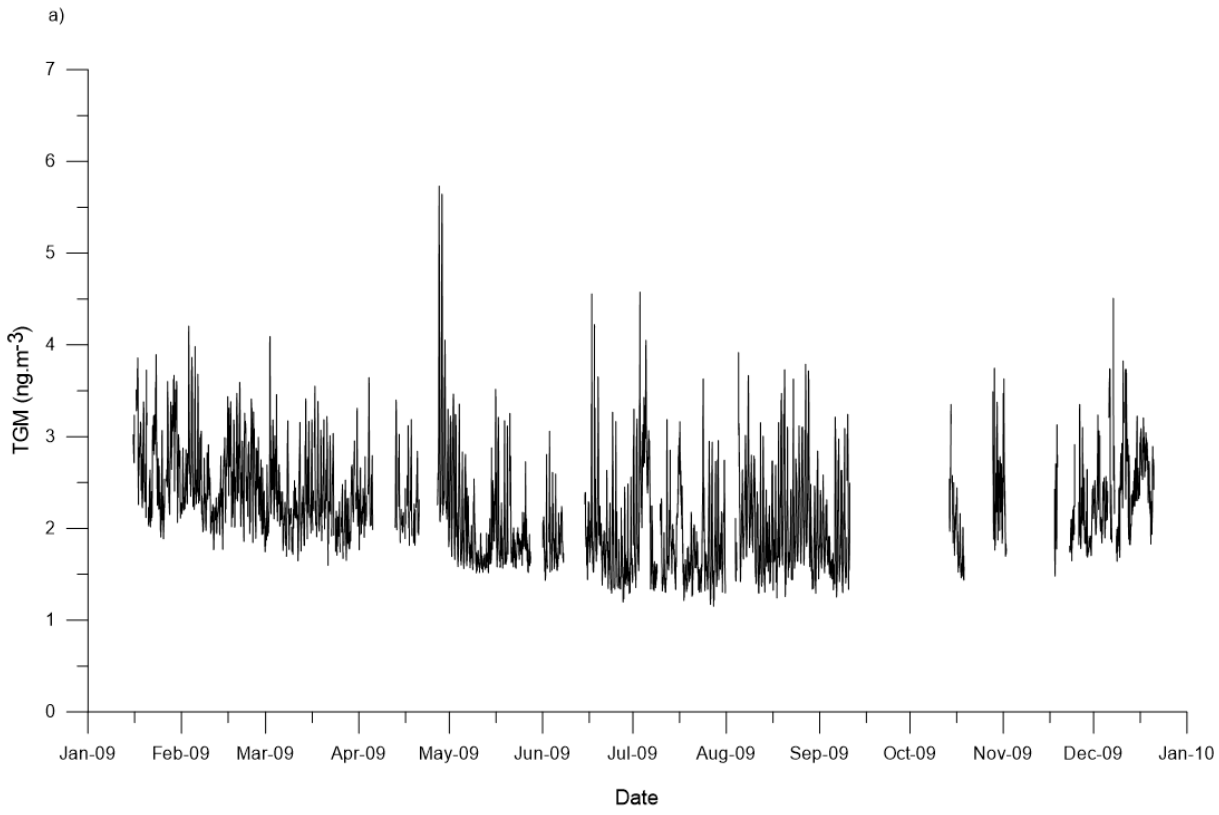

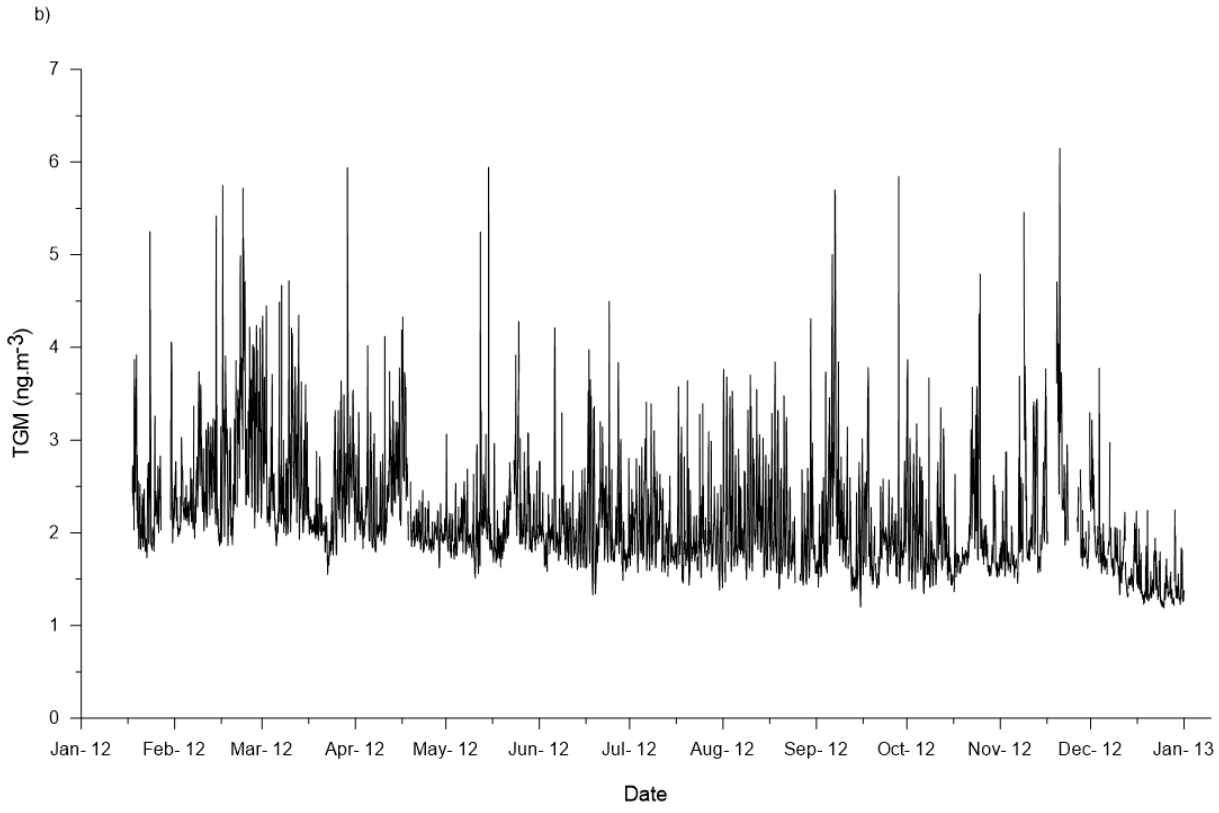

Fig.2 : TGM concentrations (hourly mean) measured at La Seyne-sur-Mer in 2009 (a) and 2012 (b).

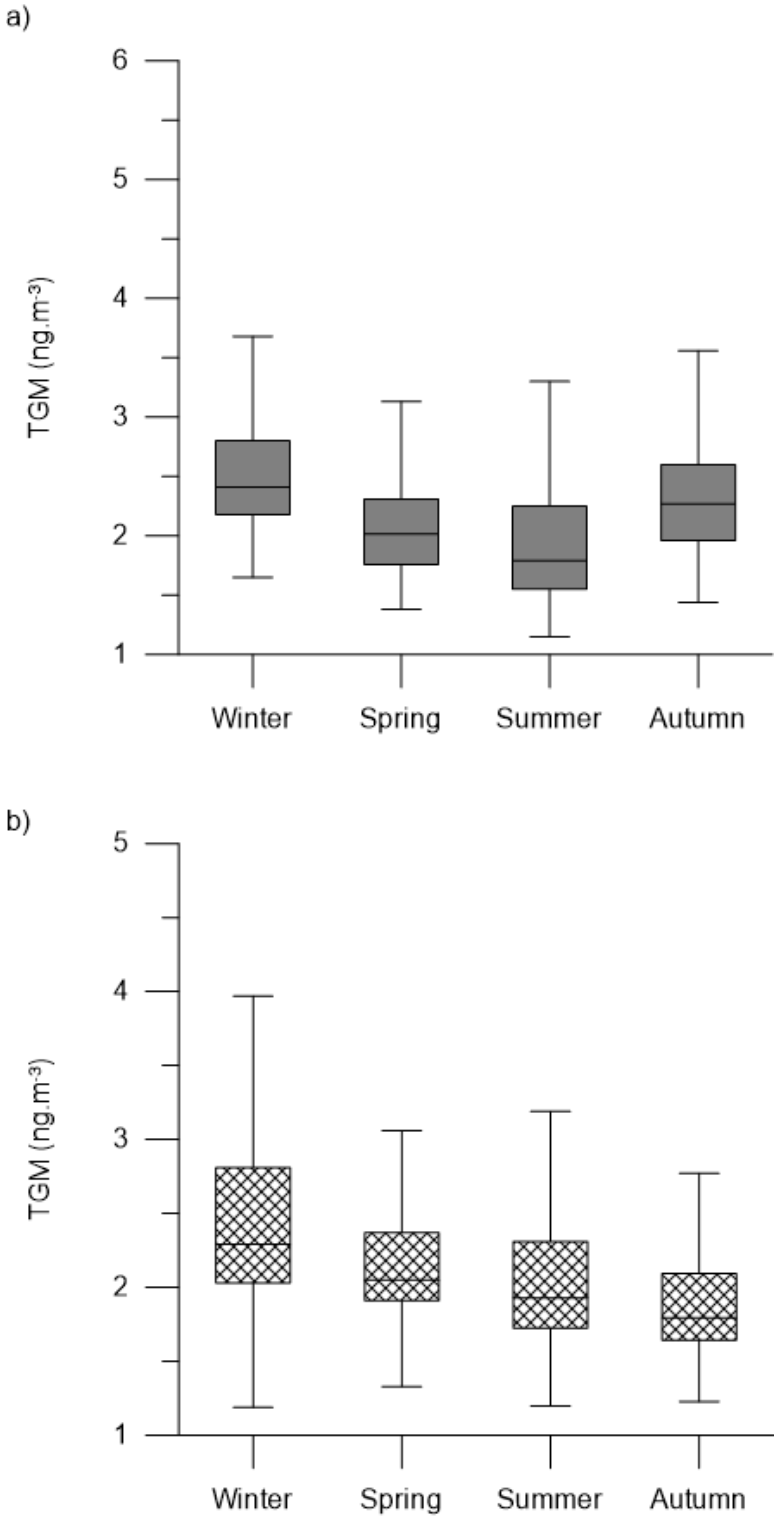

Fig.3 : Box and whisker plot of the average seasonally of TGM at La Seyne-sur-Mer in 2009 (a) and 2012 (b). Boxes extend from 25 to 75% quartiles; the middle line represents the median value. The whiskers extend from Min to Max values.

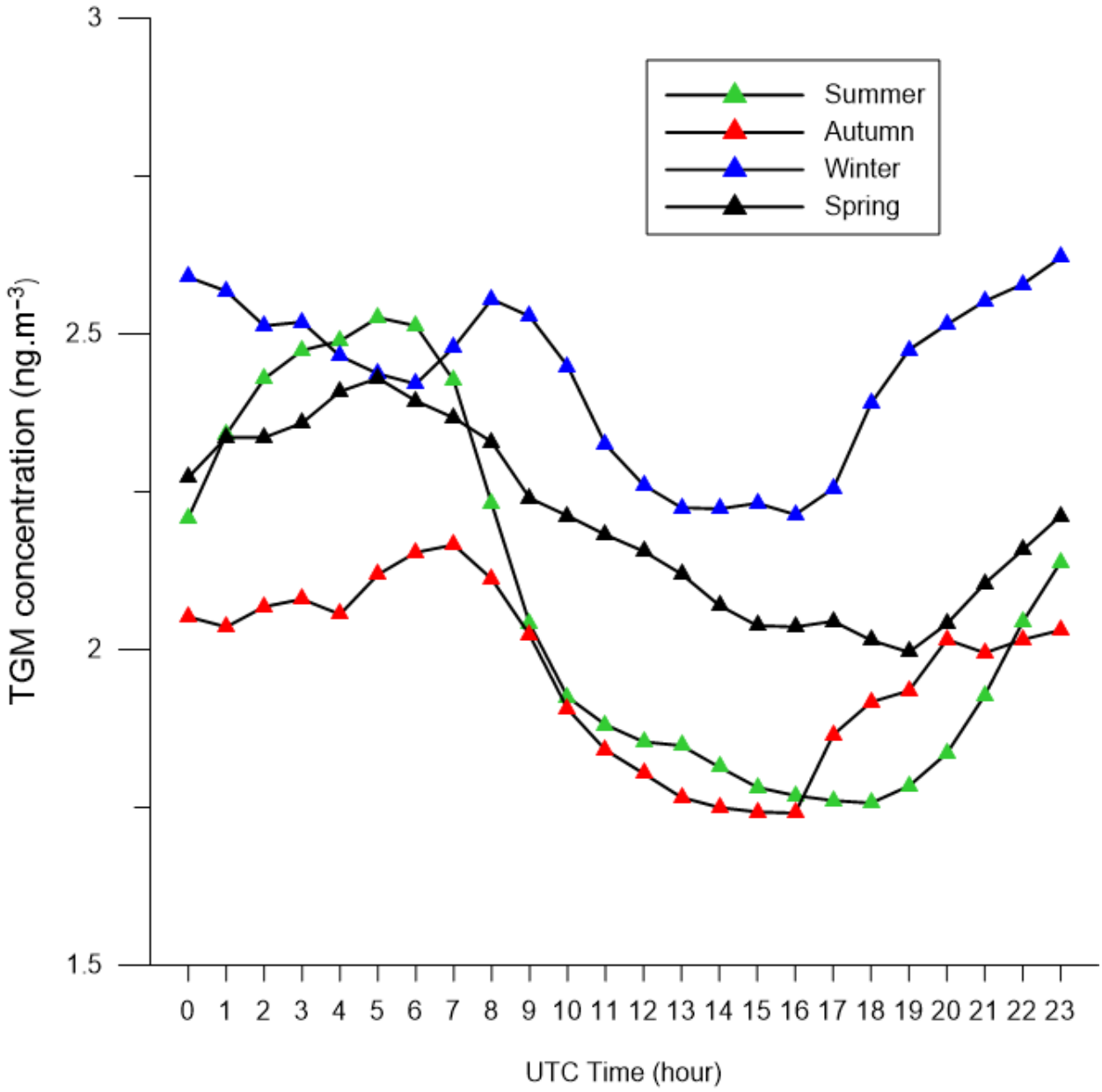

Fig. 4: Hourly variations of TGM by season at La Seyne-sur-Mer in 2012.

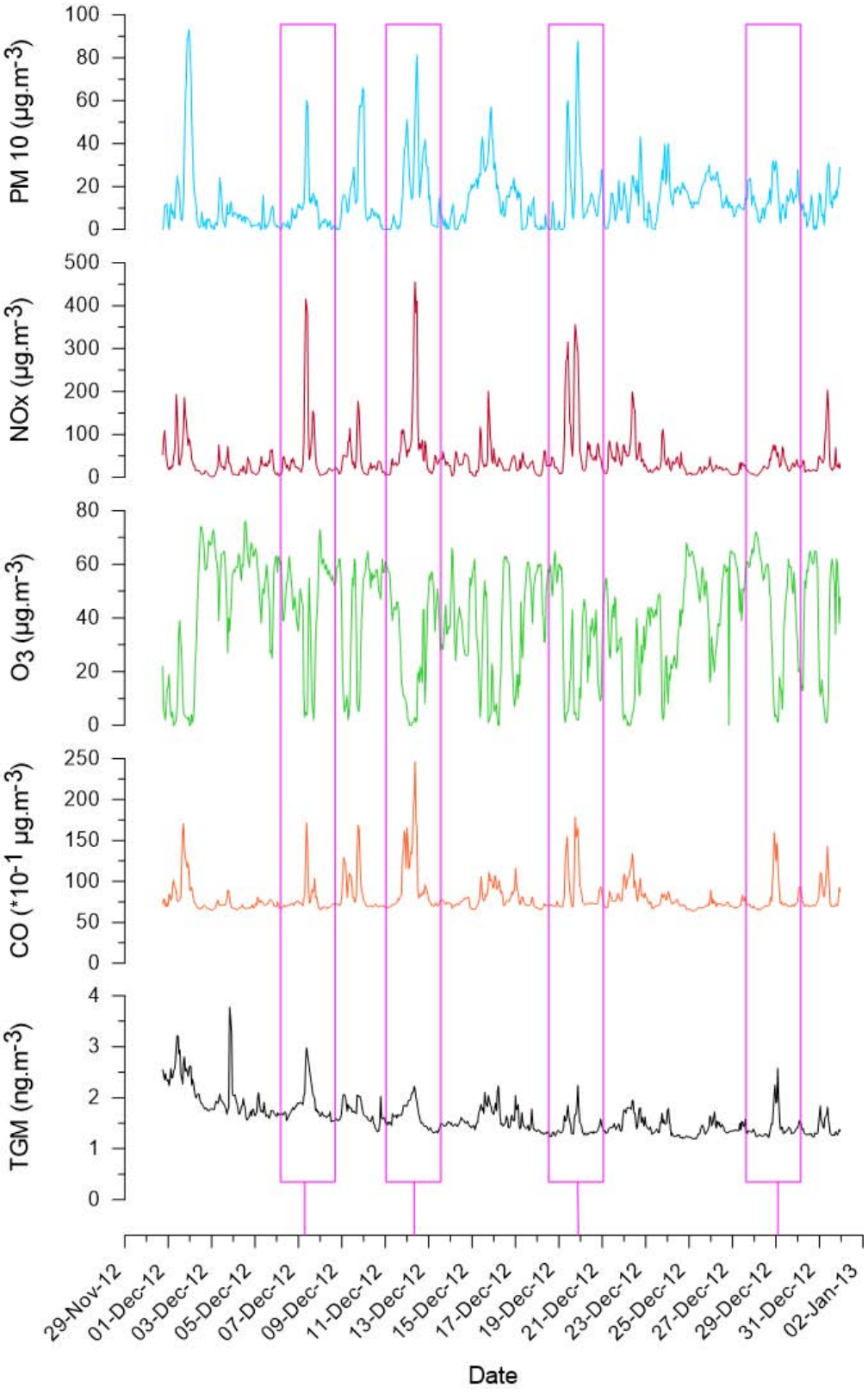

Fig.5: Comparison of TGM and pollutants variations (PM10, NOx, O_3 and CO) during December 2012. Magenta rectangles show episodes of TGM increase in relation with the others pollutants.

a)

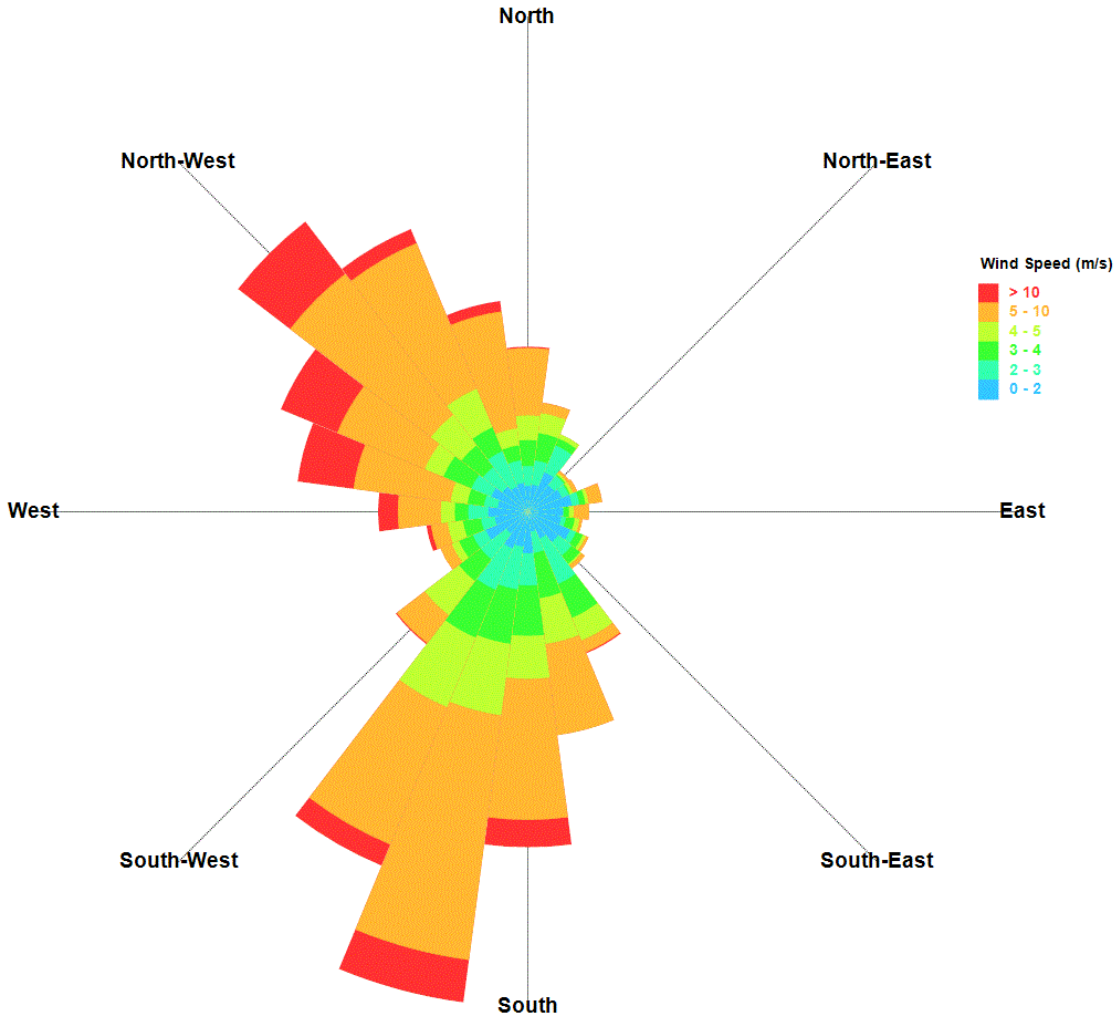

b)

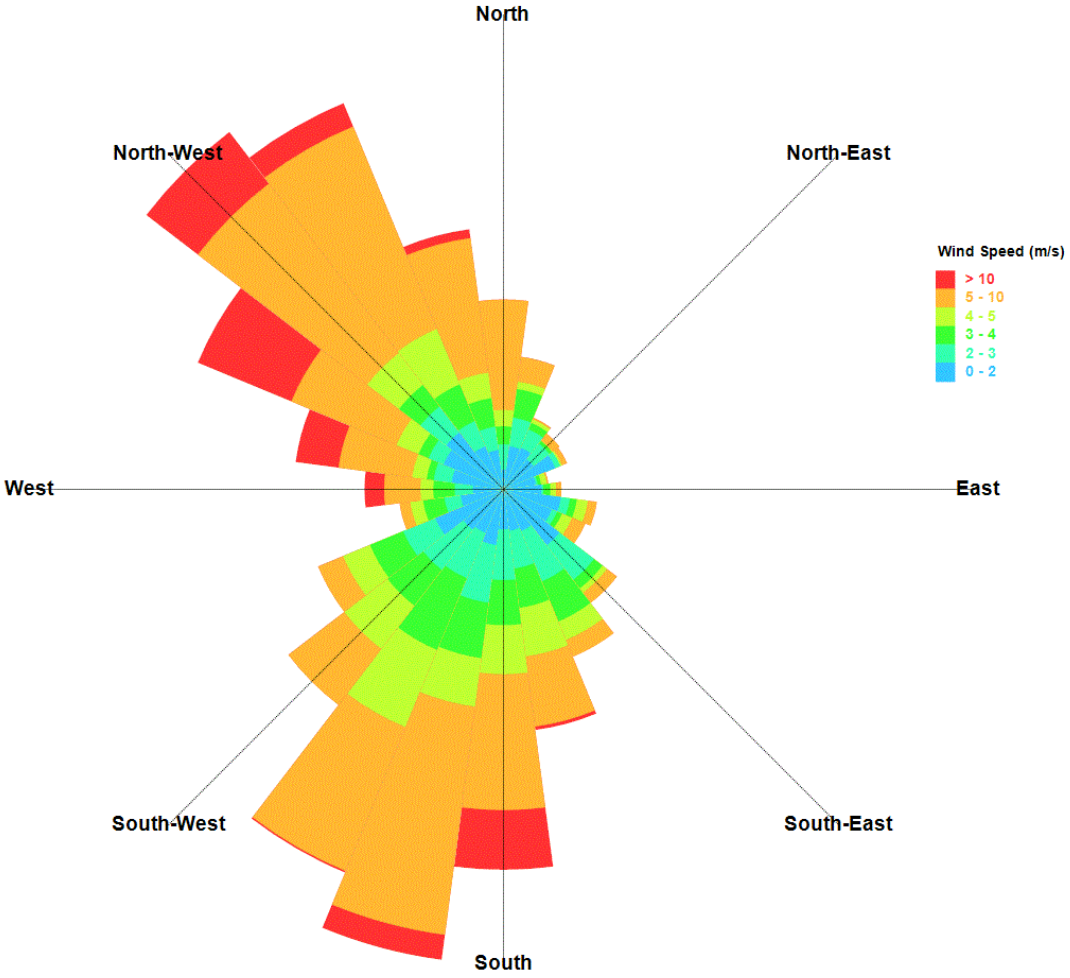

Fig 6 : Wind rose for 2009 (a) and 2012 (b)

87 a)

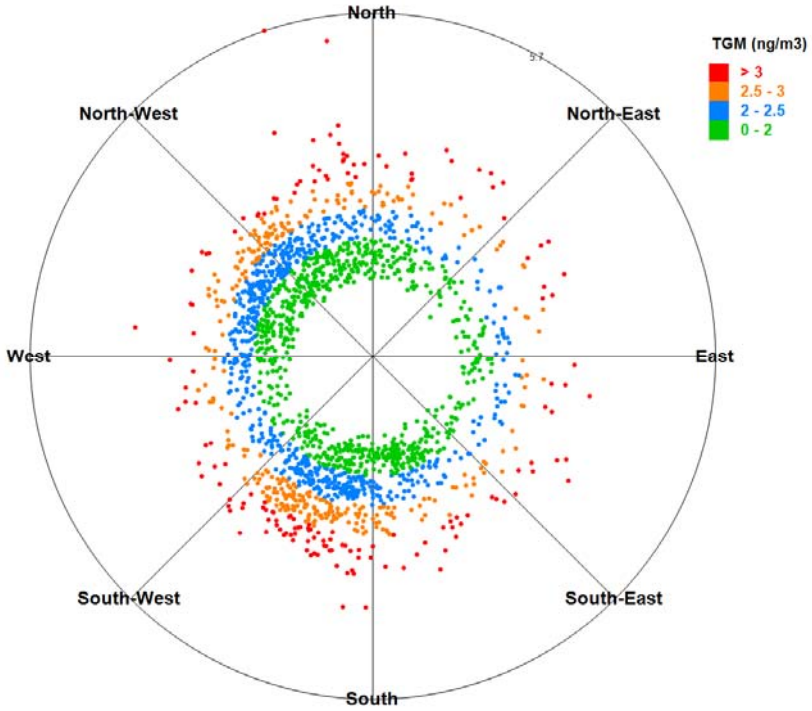

88

89

90 b)

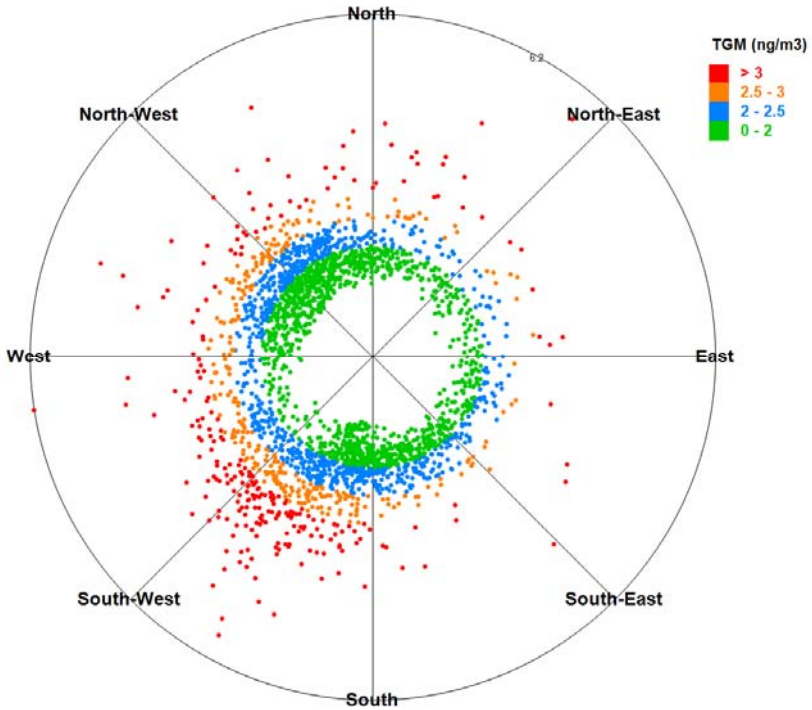

91

92

93 Fig.7: TGM rose for 2009 (a) and 2012 (b).

a)

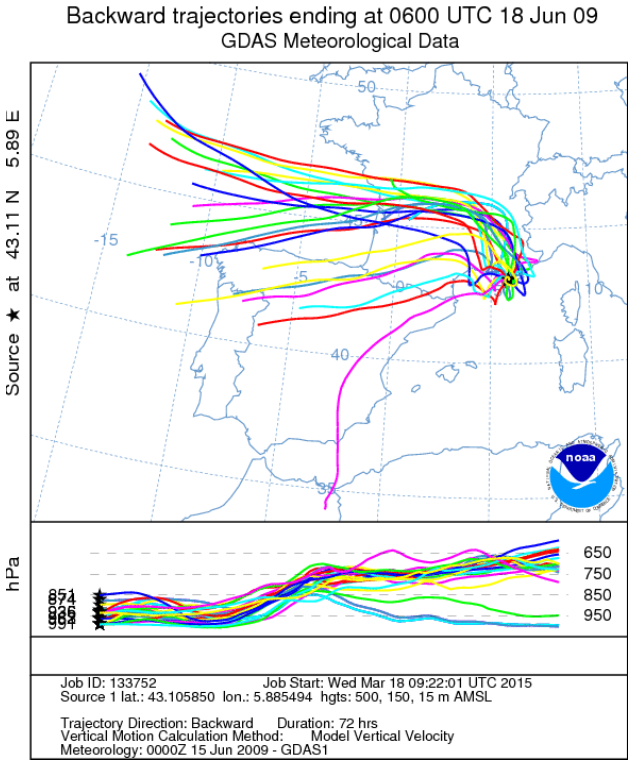
Backward trajectories ending at 0600 UTC 18 Jun 09
GDAS Meteorological Data
Source ★ at 43.11 N 5.89 E
hPa
650
750
850
950
Job ID: 133752 Job Start: Wed Mar 18 09:22:01 UTC 2015
Source 1 lat.: 43.105850 lon.: 5.885494 hgts: 500, 150, 15 m AMSL
Trajectory Direction: Backward Duration: 72 hrs
Vertical Motion Calculation Method: Model Vertical Velocity
Meteorology: 0000Z 15 Jun 2009 - GDAS1

b)

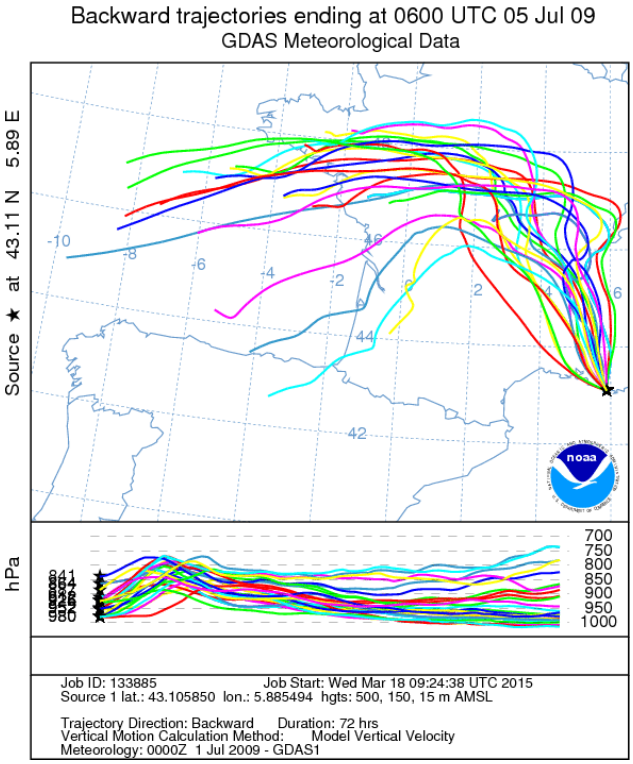
Backward trajectories ending at 0600 UTC 05 Jul 09
GDAS Meteorological Data
Source ★ at 43.11 N 5.89 E
hPa
700
750
800
850
900
950
1000
Job ID: 133885 Job Start: Wed Mar 18 09:24:38 UTC 2015
Source 1 lat.: 43.105850 lon.: 5.885494 hgts: 500, 150, 15 m AMSL
Trajectory Direction: Backward Duration: 72 hrs
Vertical Motion Calculation Method: Model Vertical Velocity
Meteorology: 0000Z 1 Jul 2009 - GDAS1

101 c)

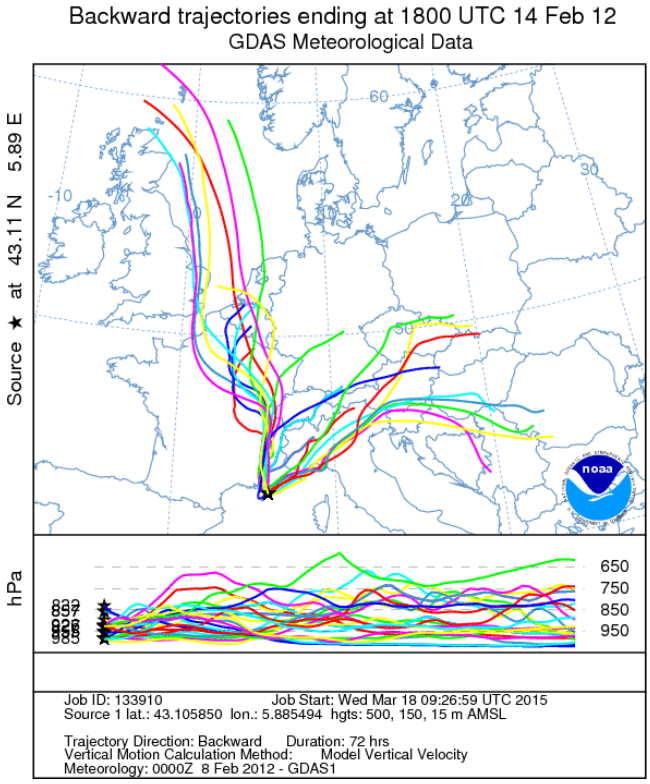

102

103 d)

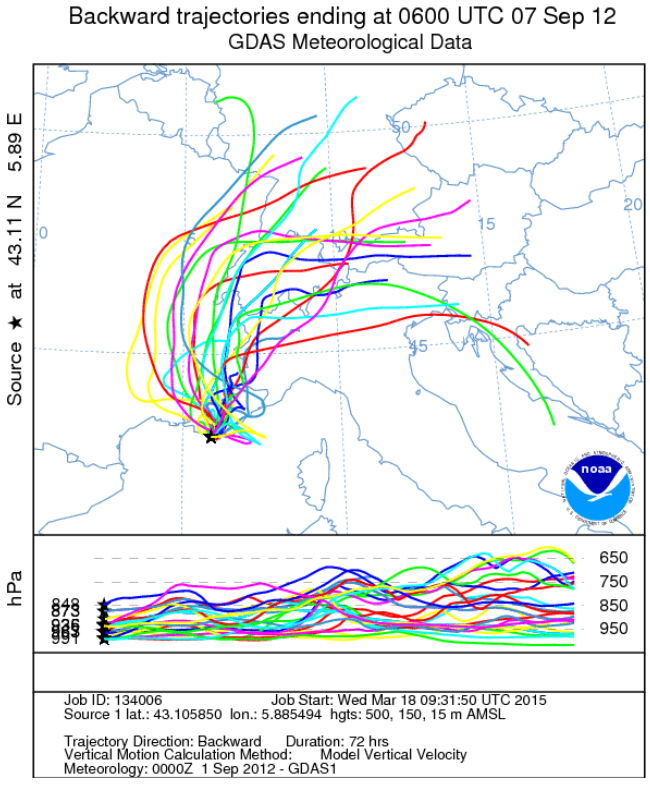

104

105 Fig.8: 3 days back-trajectories for 4 episode of high significant concentration of TGM (>3 ng.m^{-3})
106 observed for each years: a) 18th June 2009, 06:00 am; b) 05th July 2009, 06:00 am; c) 14th
107 February 2012, 06:00 pm; d) 07th September 2012).